JOURNAL OF CATALYSIS **178,** 586–597 (1998)
ARTICLE NO. CA982180

Reducibility and Adsorbate Interactions of Ti in Titanosilicate Molecular Sieve TS-1

A. M. Prakash and Larry Kevan[1]

Department of Chemistry, University of Houston, Houston, Texas 77204-5641

Received February 24, 1998; revised May 5, 1998; accepted May 21, 1998

Electron spin resonance (ESR) and electron spin echo modulation (ESEM) spectroscopy are used to study reducibility and adsorbate interaction of Ti in titanosilicate TS-1 molecular sieve. Various reduction methods were used to reduce Ti(IV) in TS-1 to Ti(III) which was then monitored by ESR. When TS-1, after dehydration and oxygen treatment at high temperature followed by evacuation (activation), is γ-irradiated at 77 K; an ESR signal with $g_{\parallel} = 1.970$ and $g_{\perp} = 1.906$ is observed for isolated Ti(III) centers. Radiation induced defect centers known as V centers are also observed after γ-irradiation. When activated TS-1 is treated with CO or H_2 at 673 K, an axial ESR signal with $g_{\perp} = 1.968$ and $g_{\parallel} = 1.933$ is observed which is suggested to be Ti(III)$(CO)_n$ and Ti(III)$(H_2)_n$ complexes. When activated TS-1 is exposed to D_2O at room temperature and subsequently γ-irradiated at 77 K, a new ESR signal with $g = 1.924$ is observed. This species is identified as Ti(III)-$(OD)_1$ from ^{2}D ESEM data. Adsorption of CH_3OD on activated TS-1 produces a new Ti(III) species with $g = 1.931$. This species is identified as Ti(III)-$(CH_3OD)_1$ from ^{2}D ESEM data. Adsorption of C_2D_4 on activated TS-1 produces a new Ti(III) species with $g_{\perp} = 1.968$ and $g_{\parallel} = 1.910$. This species is identified as Ti(III)-$(C_2D_4)_1$ from ^{2}D ESEM data. Possible coordination geometries of the various Ti(III)-adsorbate complexes are discussed.

INTRODUCTION

Since the discovery of titanosilicate molecular sieve TS-1 in the early 1980s, there has been a large scientific effort on the synthesis, characterization, and utilization of titanium-containing molecular sieves (1,2). TS-1 has proved to be an excellent catalyst for the selective oxidation of various organic substrates in the presence of hydrogen peroxide (3–6). The formation of surface titanium peroxo compounds with H_2O_2 and the subsequent transfer of the peroxidic oxygen to the organic reactants has been proposed as the mechanism by which TS-1 catalyzes the reaction. An intensive search for other compounds with properties similar to TS-1 has resulted in the syntheses of TS-2 (7), Ti-ZSM-48 (8), Ti-β (9), TAPO-5 (10), TAPO-11 (11), and TAPO-36 (11). Recently, titanium-containing mesoporous molecular sieves such as TiHMS (12), TiMCM-41 (13), and TiMCM-48 (14) have also been reported. The unusual properties of titanium silicates have been attributed to tetrahedrally coordinated titanium substituted into a SiO_2 lattice coupled with very high dispersion of the active catalytic centers resulting from such substitution. New microporous titanosilicates, named ETS-4 and ETS-10, where titanium occurs with six coordination have also been reported (15). These materials do not exhibit the catalytic properties typical of other titanium silicates in which Ti(IV) is in tetrahedral coordination.

Electron spin resonance (ESR) spectroscopy has been widely used for characterizing several transition-metal-incorporated molecular sieves. ESR characterization of Ti compounds, in general, and titanosilicates, in particular, are limited due to the fact that the most common and stable oxidation state of titanium in these materials is tetravalent which is ESR silent. However, trivalent titanium with a $3d^1$ electron configuration has characteristic ESR signals dependent on its coordination geometry. The low stability of Ti(III) at room temperature again makes it a less favorable candidate for ESR study. In order to study titanosilicate molecular sieves by ESR these materials have to be reduced by suitable reduction methods. Several reduction methods are used to reduce transition metal ions in zeolites and other molecular sieves. High temperature thermal treatment, treatment with H_2 or CO at moderate to high temperature, UV irradiation, or γ-ray irradiation are the commonly used reduction methods. Each of these reduction methods has its own merits and demerits. ESR evidence for isomorphous substitution of Ti(IV) into TS-1 has been reported (16,17). Very recently, we studied the nature of Ti in TAPO-5 and TiMCM-41 molecular sieves by ESR and electron spin echo modulation (ESEM) spectroscopy and provided convincing evidence for the framework substitution of titanium (18,19). Since the catalytic properties of titanosilicate materials are strongly dependent on the nature and location of the titanium ions and their accessibility to adsorbates and coordination with ligands, it is important to elucidate the number and orientation of their coordinating molecules. Sevaral studies using spectroscopic techniques such as IR, UV, and X-ray absorption techniques of

[1] Corresponding author. E-mail: KEVAN@UH.EDU.

0021-9517/98 $25.00

EXANES and EXAFS have been reported on the coordination properties of titanium in TS-1 in relation to their interaction with external adsorbate molecules. Although the results obtained from various studies are consistent with the idea that coordination state of titanium changes significantly after adsorption, the number of molecules coordinating to titanium deduced from these techniques do not generally agree and also are not always consistent with the models proposed from catalytic studies. Electron spin echo modulation spectroscopy combined with ESR effectively provides quantitative information concerning the adsorbate geometry in terms of the number of surrounding adsorbate nuclei (N) and their interaction distance (R). In this study we report ESR results on the reducibility of titanium in TS-1 by various reduction methods. ESEM spectroscopy has been used for the first time to elucidate the coordination geometry of Ti(III) in TS-1 with various adsorbate molecules.

EXPERIMENTAL SECTION

Preparation

TS-1 was prepared hydrothermally using tetrapropylammonium hydroxide as the organic template. The synthesis procedure is essentially same as that reported earlier (6). The following chemicals were used without further purification; tetraethylorthosilicate (98%, Aldrich), tetrapropylammonium hydroxide (20 wt% in water, Fluka), and titanium ethoxide (Aldrich). Syntheses were carried out in 100 cm^3 stainless steel reactors lined with Teflon material at autogenous pressure without agitation. Based on preliminary experiments, the following molar composition was optimized for the preparation of TS-1 : 0.03, TiO_2 : 1.00, SiO_2 : 0.36, TPA : 35, H_2O. In a typical synthesis, a solution of 0.53 g titanium ethoxide in 18.8 g tetraethylorthosilicate was added to 40.6 g 20 wt% aqueous solution of tetrapropylammonium hydroxide, while stirring. The resulting mixture was kept stirring at 333 K for 3 h. Occasionally water was added to compensate for evaporation. The final gel was crystallized at 473 K for 42 h. After crystallization the product was separated from the mother liquor by vacuum filtration, washed with water, and dried at 373 K overnight. A sample of silicalite-1 was also prepared in essentially the same procedure, except that the addition of the titanium source was omitted. Samples were calcined by heating as-synthesized samples slowly to 823 K in O_2 and kept at this temperature for 16 h for removal of the organic matter.

Sample Treatment and Measurements

Powder X-ray diffraction (XRD) patterns were recorded on a Siemens D5000 X-ray diffractometer using CuKα radiation. The spectra were collected stepwise in the $4^\circ \leq 2\theta \leq 50^\circ$ angular region with 0.005° steps and 1 s counting time. Chemical analyses of the samples were carried out by electron microprobe analysis on a Jeol JXA-8600 spectrometer. For ESR and ESEM measurements, the calcined samples were loaded into 3 mm OD by 2 mm ID Suprasil quartz tubes and evacuated to a final pressure of 10^{-4} Torr at 295 K overnight. To study the behavior of the titanium as a function of hydration, the samples were heated under vacuum from 295 to 673 K at regular intervals. For each interval, the temperature was raised slowly and held at that temperature for 16 h. Then ESR spectra were measured at 77 K to study the change by this thermal treatment. To study the reduction behavior of TS-1, the samples were dehydrated at 673 K and then contacted with 1 atm of O_2 at 673 K for 16 h, followed by evacuation at the same temperature (activation). The activated samples were contacted with 350 Torr of dry hydrogen or 40 Torr of CO at 295 K and heated to various temperatures for varying durations before ESR measurements. In another reduction procedure, activated samples were sealed and immersed in liquid nitrogen and then exposed to γ-radiation from a ^{60}Co source at 77 K to a total dose of 1.6 Mrad at a dose rate of 0.20 Mrad h^{-1}. In order to prepare Ti(III) complexes with various adsorbates the activated samples were exposed to the room temperature vapor pressure of D_2O (Aldrich Chemical), CH_3OD (Stohler Isotope Chemicals), and 10 Torr C_2D_4 (Cambridge Isotope Laboratories). These samples with adsorbates were sealed and kept at room temperature for 24 h before exposing to γ-radiation at 77 K to a total dose of 1.6 Mrad.

ESR spectra were recorded with a Bruker ESP 300 X-band spectrometer at 77 K. The magnetic field was calibrated with a Varian E-500 gaussmeter. The microwave frequency was measured by a Hewlett Packard HP 5342A frequency counter. ESEM spectra were measured at 4.8 K with a Bruker ESP 380 pulsed ESR spectrometer. Three pulse echoes were measured by using a $\pi/2\text{-}\tau\text{-}\pi/2\text{-}T\text{-}\pi/2$ pulse sequence as a function of time T to obtain the time domain spectrum. To minimize ^{29}Si modulation in measurements of deuterium modulation, the τ value was fixed accordingly, depending on the magnetic field position. The deuterium modulation was analyzed by a spherical approximation for powder samples in terms of N nuclei at distance R with an isotopic hyperfine coupling A_{iso} (20). The best fit simulation of an ESEM signal is found by varying the parameters until the sum of the squared residuals is minimized.

RESULTS

Powder X-Ray Diffraction

Both TS-1 and silicalite-1 were characterized by XRD. Figure 1 shows the powder XRD patterns of as-synthesized TS-1 and silicalite-1. These patterns, both in intensity and line position, match well with the patterns reported for the two compositional variants of the MFI structure type (21). The change from the monoclinic structure of silicalite-1 to

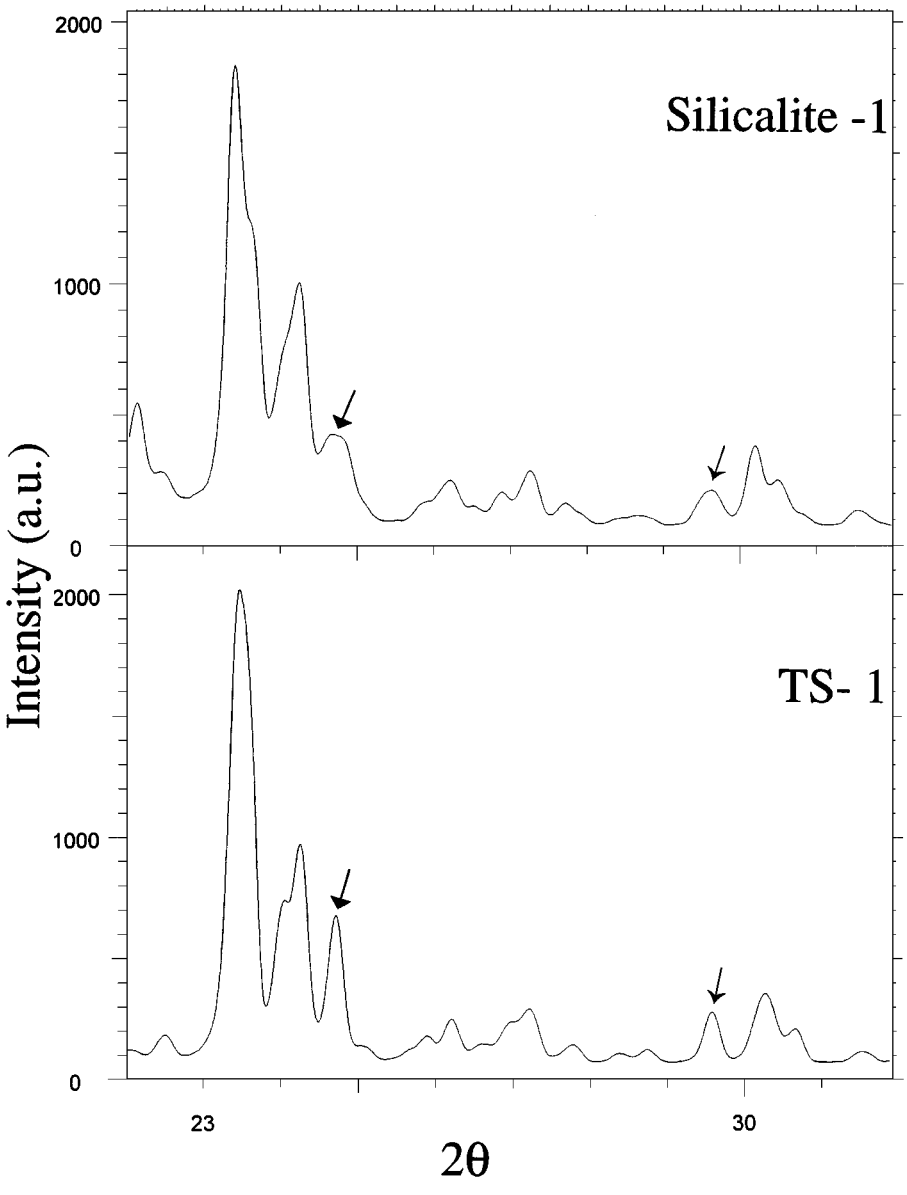

FIG. 1. X-ray powder diffraction pattern for (a) TS-1 and (b) silicalite-1 in their calcined forms. The arrows indicate that lines at $2\theta = 24.4^\circ$ and 29.3° in TS-1 are changed to doublets in silicalite-1 due to a change of crystal symmetry from orthorhombic (TS-1) to monoclinic (silicalite-1).

the orthorhombic structure of TS-1 is evident from the splitting of lines at 24.4° and 29.3° observed in the former. This is cited as strong evidence for the incorporation of Ti into the silicalite framework (21).

Elemental Analysis

Electron microprobe analysis of TS-1 gives a Si/Ti ratio of 66. This corresponds to about 1.5 titanium ions per unit cell of TS-1. A maximum limit of 2.3 Ti per unit cell is reported in the literature for TS-1 without forming any TiO_2 phase. Since the observed value in our sample is well below the maximum limit, we assume that all titaniums in our sample are in framework sites.

Electron Spin Resonance

Calcined, hydrated TS-1 does not show any ESR signal at 77 K. Thus, we assume that the Ti species exist in the form of Ti(IV). Dehydration at temperatures up to 673 K does not show any ESR signal. Under the same treatment silicalite-1 also does not show any ESR signal.

Isolated Ti(III) ions in TS-1 can be generated by γ-ray irradiation at 77 K. Figure 2 shows ESR spectra at 77 K after γ-ray irradiation of activated TS-1 and silicalite-1. The γ-irradiation at 77 K shows a strong rhombic signal around $g = 2$ due to radiation induced defect centers known as V centers and an axial signal with $g_{\parallel} = 1.970$ and $g_{\perp} = 1.90$ due

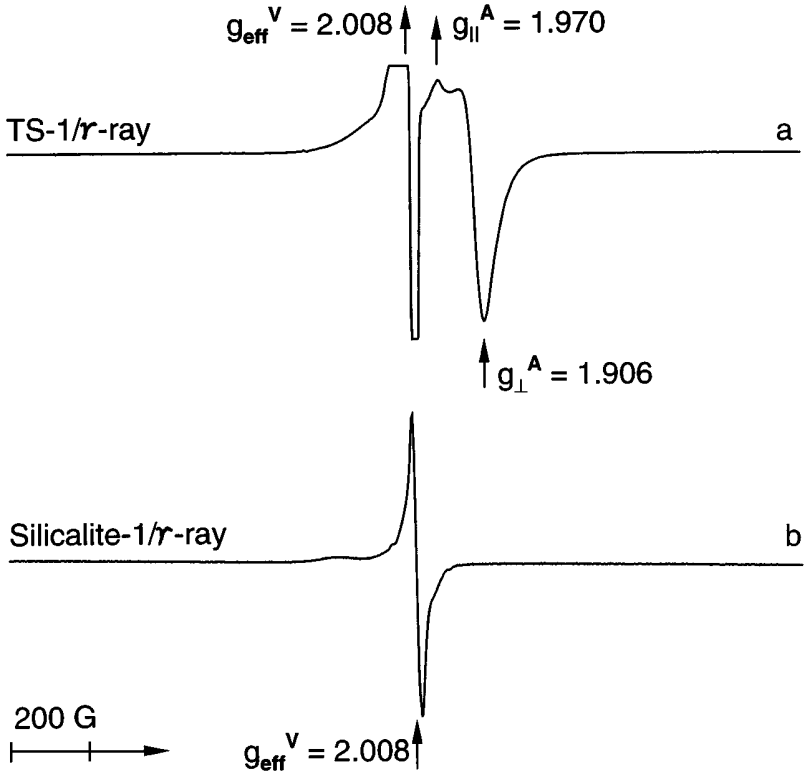

FIG. 2. ESR spectra at 77 K of (a) TS-1 and (b) silicalite-1 after γ-irradiation at 77 K of activated samples.

to Ti(III) centers. The latter assignment is based on the fact that when silicalite-1 is γ-irradiated, only a signal due to V centers is observed. The observed axial signal for Ti(III) in TS-1 closely similar to the signal observed in TiMCM-41 and indicates similar crystalline symmetry for this ion in these two materials (19).

Figure 3 shows the ESR spectra of TS-1 after hydrogen and CO treatment at 673 K. Almost similar signals with axially symmetric g tensors (species B with $g_{\parallel} = 1.933$ and $g_{\perp} = 1.968$ for CO and species C with $g_{\parallel} = 1.931$ and $g_{\perp} = 1.962$ for H_2) are observed. We assign these signals to Ti(III) species modified by interactions from CO or H_2 molecules or interactions from the corresponding oxidized species formed as a consequence of the reductive process. The ESR signal intensity for species A produced by γ-irradiation is substantially higher than the signal intensity observed for species B and C after carbon monoxide or hydrogen treatment. When TS-1 samples with CO or H_2 are outgassed at room temperature for about 5 min, the ESR intensity of the Ti(III) species is reduced from its original intensity. The reduction in intensity is probably due to the reoxidation of Ti(III) to Ti(IV) upon removal of the ligands. However, due to the inherent instability of the Ti(III) species at room temperature, the reversible nature of the Ti(III) signal in the presence and absence of CO or H_2 molecules was not able to be studied.

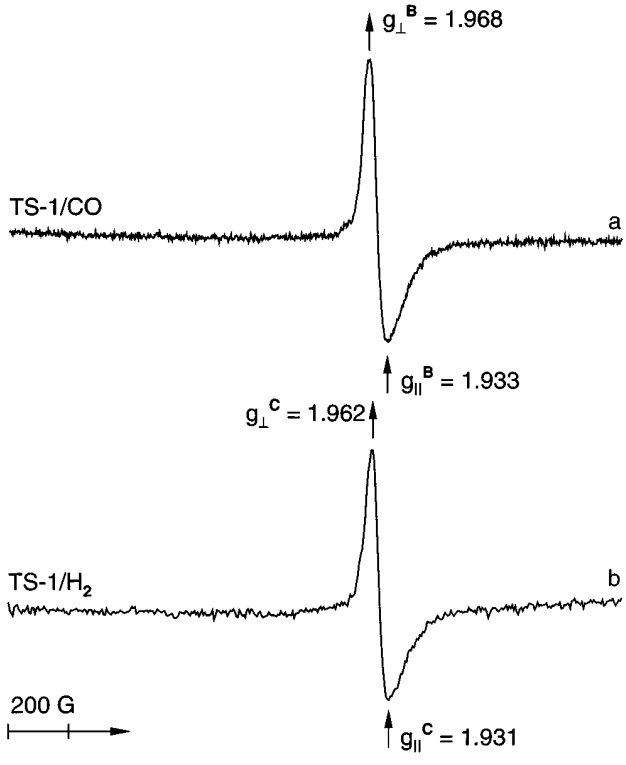

FIG. 3. ESR spectra at 77 K of TS-1 after treatment with (a) CO and (b) H_2 at 673 K.

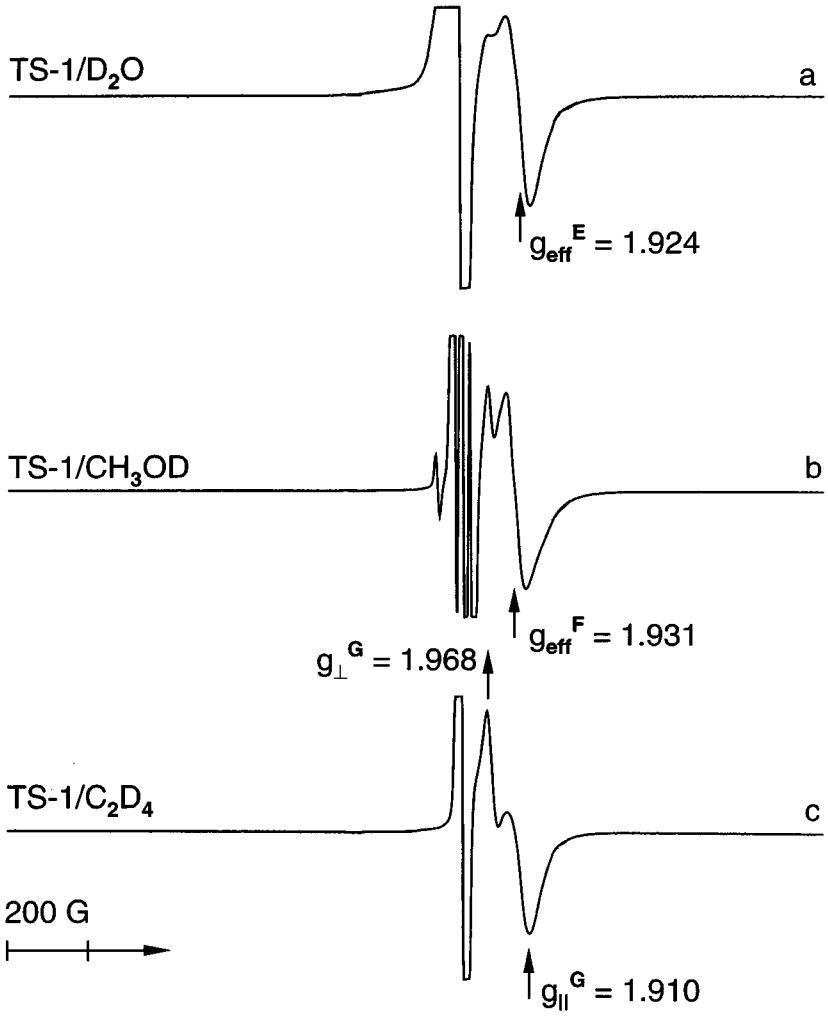

FIG. 4. ESR spectra at 77 K of TS-1 after adsorption of (a) D_2O, (b) CH_3OD, and (c) C_2D_4 and subsequent γ-irradiation at 77 K, followed by annealing at 295 K for a short time.

Figure 4 shows the ESR spectra obtained for TS-1 after D_2O, CH_3OD, and C_2D_4 adsorption, followed by γ-irradiation at 77 K. D_2O adsorption on TS-1 produces a new Ti(III) species E characterized by a slightly anisotropic signal with $g = 1.924$. Adsorption of CH_3OD at room temperature on TS-1 leads to the formation of Ti(III) species F (Fig. 4b), characterized by an anisotropic signal with $g = 1.931$. Note that signals for both species E and F are anisotropic to almost the same extent and have similar g values, indicating similar crystalline environments for the Ti(III) ion after the adsorption of D_2O and CH_3OD. The V center observed with adsorbed CH_3OD is much more complex than the V center observed in TS-1 after D_2O adsorption. When deuterated ethylene is adsorbed on activated TS-1 and γ-irradiated, the major signal observed is a new Ti(III) species G with $g_\perp = 1.968$ and $g_\parallel = 1.910$. The ESR parameters of various Ti(III) species and their possible assignments are listed in Table 1.

The adsorption experiments involve irradiation in the presence of a gas phase which is different from simple adsorption measurements. This is especially apparent from the more complex ESR signal observed at $g \approx 2.000$ in samples containing methanol (Fig. 4d). Such an approach seems un-

TABLE 1

ESR Parameters of Various Ti(III) Species Observed in TS-1 Molecular Sieves

Treatment	Species	Assignment	$g_\parallel$	g_{eff}	$g_\perp$
γ-irradiation/77 K	A	Ti(III)	1.970		1.906
CO/673 K	B	$Ti(III)(CO)_n$	1.933		1.968
H_2/673 K	C	$Ti(III)(H_2)_n$	1.931		1.962
D_2O	E	$Ti(III)(OD)_1$		1.924	
CH_3OD	F	$Ti(III)(CH_3OD)_1$		1.931	
C_2D_4	G	$Ti(III)(C_2D_4)_1$	1.910		1.968

avoidable due to the inherent instability of Ti(III) in TS-1 at room temperature, coupled with the practical limitations of the experimental setup. A similar approach was adopted earlier in studies involving the unstable oxidation state of several transition metals. The fact that γ-irradiation did not produce any paramagnetic species having ESR signals in the region where Ti(III) appears still makes this procedure useful to study Ti(III) complexes with various adsorbate molecules.

Three-pulse ^{2}D ESEM spectra were recorded at the magnetic field corresponding to the Ti(III) species observed after adsorption of various deuterated adsorbates. The delay between the first and second pulses (τ) was selected, depending on the magnetic field so as to minimize modulation from other magnetic nuclei present in the system. Figure 5 shows the ^{2}D ESEM spectrum of TS-1 after adsorbing D_2O. The magnetic field was set at the center of species E (Fig. 3a). Simulation of the spectrum gives one deuterium nucleus at a distance of 3.0 Å and a second deuterium nucleus at 3.5 Å. These values are consistent with one OD group coordinating directly with Ti(III) and another OD group interacting from a farther distance. Figure 6 shows the experimental and simulated ^{2}D ESEM spectrum of TS-1 after adsorbing CD_3OH. The field was set at the center of species F (Fig. 3b). The spectrum was simulated with one deuterium nucleus at 2.8 Å. These parameters can be rationalized in terms of one methanol molecule having direct coordination with the Ti(III) ion. In Fig. 7 the experimental and simulated ^{2}D ESEM spectra observed for TS-1 after adsorbing C_2D_4 are given. The field was set at $g_\parallel$ of species G (Fig. 4c). Simulation of the spectrum gives four deuterium nuclei at 4.5 Å, indicating one molecule of ethylene coordinating with Ti(III) to form species G.

DISCUSSION

Gamma irradiation of activated TS-1 produces two ESR signals besides the doublet signal due to atomic hydrogen. The strong signal with $g_1 = 2.015$, $g_2 = 2.007$, and $g_3 = 1.999$ is clearly assigned to V centers created by irradiation. A similar signal is observed in silicalite-1, although with lesser intensity. V centers in zeolite and other molecular sieves have been studied earlier (22,23). In zeolites two types of V centers, namely V_1 and V_2 centers associated with Al-O-Si and Si-O-Si units of the framework, have been identified. These are radiation-induced hole centers trapped in a lone pair p orbital of associated oxygen atoms. Also V centers have been reported recently in aluminophosphate materials and mesoporous MCM-41 materials (18,19). Unlike zeolites, since there is no Al-O-Si unit present in silicalite-1, only one type of V center associated with a Si-O-Si unit is expected.

The second signal with $g_\parallel = 1.970$ and $g_\perp = 1.906$ is assigned to Ti(III) produced by reduction of Ti(IV) by

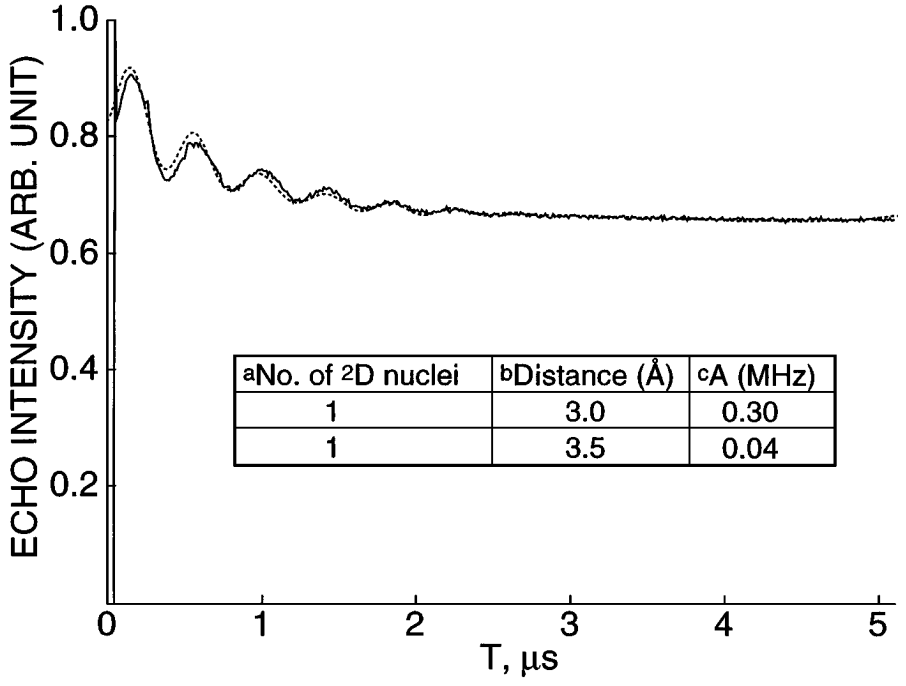

FIG. 5. Experimental (———) and simulated (...) ^{2}D ESEM spectra of TS-1 after adsorption of D_2O and γ- irradiation at 77 K. The spectrum was recorded at the magnetic field corresponding to the center of Ti(III) species E. (a) Number of deuterium nuclei interacting with Ti(III). (b) Distance between deuterium and Ti(III); estimated uncertainty is ±0.01 nm. (c) Isotopic hyperfine coupling constant; estimated uncertainty is ±10%.

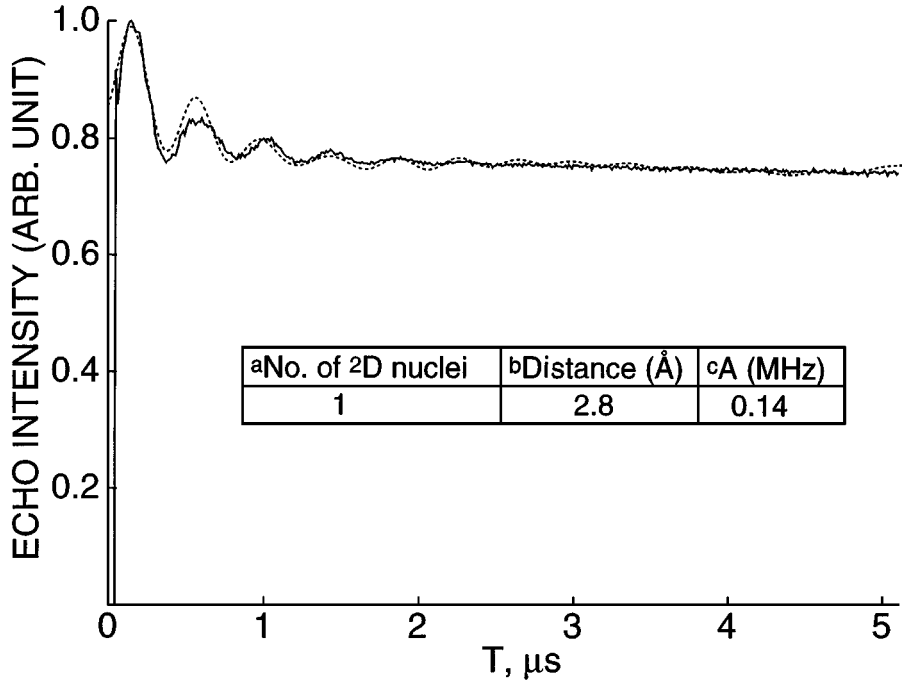

FIG. 6. Experimental (———) and simulated (…) ^{2}D ESEM spectra of TS-1 after adsorption of CH_3OD and γ- irradiation at 77 K. The spectrum was recorded at the magnetic field corresponding to the center of Ti(III) species F. (a) Number of deuterium nuclei interacting with Ti(III). (b) Distance between Ti(III) and deuterium; estimated uncertainty is ±0.01 nm. (c) Isotopic hyperfine coupling constant; estimated uncertainty is ±10%.

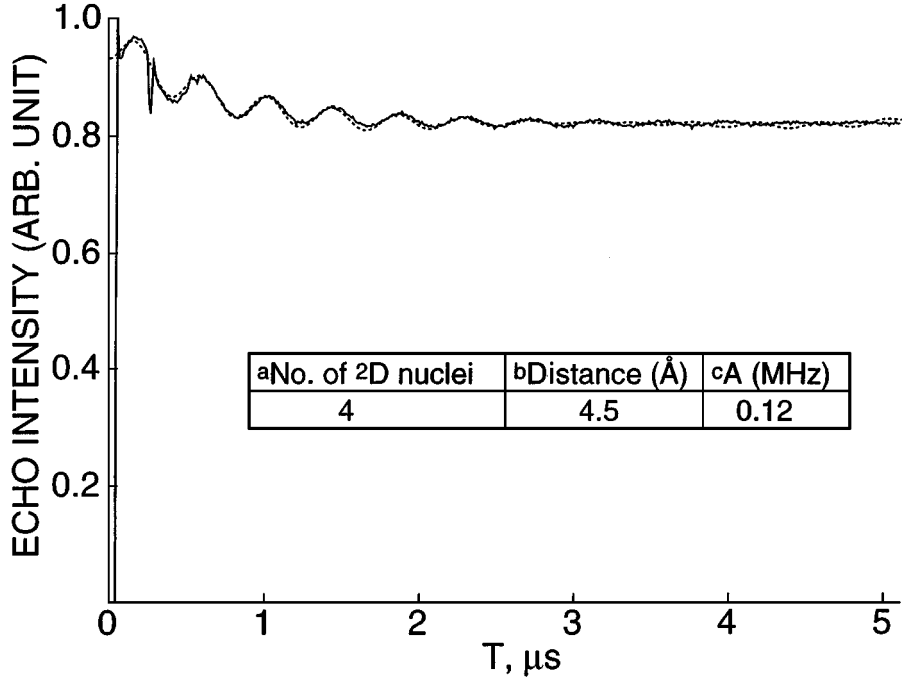

FIG. 7. Experimental (———) and simulated (…) ^{2}D ESEM spectra at 4.8 K of TS-1 after adsorption of C_2D_4 and γ- irradiation at 77 K. The spectrum was recorded at the magnetic field corresponding to the parallel component of Ti(III) species G. (a) Number of deuterium nuclei interacting with Ti(III). (b) Distance between Ti(III) and deuterium; estimated uncertainty is ±0.01 nm. (c) Isotopic hyperfine coupling constant; estimated uncertainty is ±10%.

electrons produced by γ-irradiation. This is supported primarily by the fact that no similar signal is produced when silicalite-1 is subjected to γ-irradiation. Second, the observed signal is in the same region where Ti(III) has been reported to have an ESR signal in several titanium-containing materials, although the g values and the symmetry of these signals vary considerable, depending on the specific crystalline field environment. Moreover, the Ti(III) signal cannot be assigned to any carbonaceous paramagnetic species or to any nitric or nitrous oxide species which might be reasonably formed during calcination as there are no similar species observed in silicalite. All those paramagnetic species have different characteristic ESR signals. Our assignment is further supported by the fact that titanosilicate molecular sieve TiMCM-41 shows a very similar signal after γ-irradiation (19). In TiMCM-41 material having low titanium content, titanium is believed to be located at a framework tetrahedral site, as evidenced by several characterization results including ESR. However, in TiMCM-41 with relatively high titanium content, both tetrahedral and octahedral titanium is detected by ESR and diffuse reflectance ultraviolet spectroscopy.

Ghorbel et al. have reported (17) the ESR spectrum of TS-1 after UV irradiation of an activated sample. With the exception of a signal at $g = 1.92$, the reported spectrum is different from the spectrum observed for TS-1 after gamma irradiation. The various signals assigned to Ti(III) are different from the present assignment. The assignment of a signal at $g = 1.999$ as a parallel component of Ti(III) is inconsistent for an axially symmetric species. Generally a value much lower than 1.999 is reported for Ti(III) in other titanium containing compounds. Careful analysis of the linewidth and amplitude of the signal clearly shows a different paramagnetic origin for this signal. It is well known that the parallel component of an axially symmetric species has a broader linewidth and a smaller amplitude than the corresponding perpendicular component. However, the linewidth of the parallel component is about 5 G while that of the perpendicular component is more than 20 G which is inconsistent for an axially symmetric species. The linewidth and g value of this signal is more consistent for a radical or defect site generated in the system due to UV irradiation. Moreover, the spectrum shows a broad signal at about $g = 1.97$ which can be assigned to the parallel component of Ti(III) for which the perpendicular component is assigned at $g = 1.92$. Such a reassignment is very close to the signal observed in this study for Ti(III) formed after γ-irradiation.

The ESR spectrum observed in TS-1 after γ-irradiation is different from that observed in other titanosilicate molecular sieves such as ETS-4 and ETS-10, where titanium is in six coordination (24). A strong, sharp orthorhombic signal with $g_1 = 1.944$, $g_2 = 1.916$, and $g_3 = 1.862$ is observed in ETS-10. The signal is assigned to Ti(III) centers in framework TiO_6 units. The observed spectrum in TS-1 is also different from that observed in alkali titanate materials, where titanium has distorted octahedral coordination (25). In alkali titanates, more than one Ti(III) center is observed after γ-irradiation. A broad signal with $g_\perp = 1.975$ and $g_\parallel = 1.890$ and a sharp signal with $g_\perp = 1.990$ and $g_\parallel = 1.981$ occur. They are identified as Ti(III) centers formed in TiO_6 units having one and two nonbridging oxygens, respectively.

The reversed g components of the Ti(III) ions in TS-1 can be correlated to the specific crystalline field to which the ion is subjected. If titanium in TS-1 occupies a framework site, tetrahedral site symmetry is expected for Ti(III) in dehydrated TS-1. However, one cannot rule out the possibility of Ti having additional coordination with extraframework molecules like water and/or hydroxyl. In fact, higher coordination or a modification of the tetrahedral crystalline field for Ti(III) is almost always observed when extraframework species are present. The ground state of Ti(III) with a $3d^1$ configuration is ^2D. When this ion is subjected to a perfect cubic crystalline field from tetrahedral or octahedral coordination, its fivefold degeneracy is lifted in to a doublet and a triplet. In a tetrahedral field, the doublet lies lower in energy, while in an octahedral field the triplet has lower energy (26). But, the experimentally observed anisotropy and g value shift from the free electron value cannot be explained by perfect cubic symmetry. An additional trigonal or tetragonal distortion is necessary to lift the degeneracy of the low-lying doublet (tetrahedral) or triplet (octahedral) and is responsible for the g anisotropy and the deviation of g_{avg} from the free electron value $g_e = 2.0023$. In a tetragonally distorted tetrahedral field, the g values calculated to first order are (26)

$$g_\parallel \approx g_e, \quad g_\perp \approx g_e - 6\lambda/\Delta \quad \text{(tetragonal compression)}$$

and

$$g_\parallel \approx g_e - 8\lambda/\Delta, \quad g_\perp \approx g_e - 2\lambda/\Delta$$

(tetragonal elongation),

where λ is the spin orbit constant and Δ is the energy splitting between the degenerate triplet and doublet levels in a cubic tetrahedral field. From the ordering of the g values observed for Ti(III) in TS-1 after γ-irradiation, the most likely situation is one of tetragonal compression. However, there is wide variation in the values reported for the ESR parameters of Ti(III) in various compounds (27).

For the Ti(III) ion in tetragonally distorted octahedral symmetry, the g values to first order are (26)

$$g_\parallel \approx g_e - 8\lambda/\Delta, \quad g_\perp \approx g_e - 2\lambda/\delta,$$

where Δ is the energy splitting between the degenerate triplet and doublet levels in an octahedral cubic field and δ is the energy splitting within the lower triplet level under

tetragonal distortion. Using values of $\Delta = 11{,}000\ cm^{-1}$ and $\delta = 10{,}000\ cm^{-1}$ for tetragonally distorted octahedral Ti(III) ion as in alkali titanate glass (25) and $\lambda = 154\ cm^{-1}$ for Ti, the calculated g values are $g_{\|} = 1.890$ and $g_{\perp} = 1.971$.

Note that when changing from a tetrahedral crystalline field with tetragonal compression to an octahedral crystalline field, the corresponding ESR signal reverses its g components. It should be noted that the ESR signals of Ti(III) in TS-1 reverses its g components after reduction by γ-irradiation and after CO or H_2 reduction. Again the g values for Ti(III) in TS-1 after CO or H_2 reduction are comparable with the g values calculated for this ion in an octahedral crystal field. Thus, it is reasonable to conclude that after high temperature reduction with CO or H_2, Ti(III) in TS-1 is in a crystal field modified by interaction with these molecules or the corresponding oxidized species formed as a consequence of the reductive process. In support of this argument, very similar ESR spectra occur for Ti(III) impurity in alkali silicates and phosphates, where Ti(III) is surrounded by octahedrally coordinated oxygen ions (28). Ti(III) in the TS-1 framework can have additional interaction with one or two molecules of CO or H_2 and thereby acquire coordination higher than tetrahedral. The exact coordination number is still unclear. ESEM measurements are not of much help in this respect. The presence of hydrogen in the Ti(III) coordination sphere is observable by ESEM in principle, but quantitative analysis is not practically possible because of the very fast modulation from this nucleus. The spin zero ^{12}C does not have any modulation on the titanium signal.

A different ESR spectrum for Ti(III) has been reported earlier in TS-1 after treatment with CO at high temperature (673 K) (16). An axially symmetric signal with two parallel components ($g_{\|}^1 = 1.98$ and $g_{\|}^2 = 1.97$) and a common perpendicular component ($g_{\perp} = 1.193$) has been reported. This signal was interpreted as Ti(III) situated at two different tetrahedral framework sites. However, in view of our present observations and careful analysis of the line shape and g values of the reported spectrum, it seems more likely that the spectrum is composed of more than one Ti(III) species. These are probably isolated Ti(III) centers in a tetrahedral environment and a Ti(III)$(CO)_n$ complex similar to that observed here. The value of n is most likely one or two. Our argument is based on two observations. The major parallel component at $g = 1.970$ is also observed in TS-1 after γ-irradiation, but not in samples containing CO. After CO reduction we observed only one anisotropic signal which lies in the same region, where the perpendicular g component of tetrahedral Ti(III) is observed both after CO reduction in the earlier study (16) and after γ-ray reduction in this study. The relatively high concentration of CO (40 Torr) used in this study, compared to the low CO concentration in the earlier study, may be responsible for this difference in behavior.

V centers are observed in both TS-1 and silicalite-1 after γ-irradiation. The shift in V center g value from g_e is an indication of the extent of spin–orbit coupling. The shift is negative for an unpaired electron and positive for a hole. The positive shift $\Delta g = 0.005$ observed in the present case is consistent with hole trapping. This indicates that the paramagnetic center responsible for the V center is a hole and not an electron. The fact that no saturation effect with the available microwave power is observed for the V center further indicates that the defects are associated with the framework. On the other hand, a saturation effect is expected if the V centers are due to trapped electrons or holes at lattice defects. It has been observed that the stability of V centers in zeolites is strongly dependent on the presence of electron scavengers such as H^+ or Na^+ (22). The intensity of V centers produced in TS-1 is larger than the corresponding intensity in siliceous silicalite-1. A reaction mechanism for the formation of V centers in zeolites, mesoporous materials, and aluminophosphates has been proposed earlier (18,19,23). Following that interpretation, the formation of V centers in TS-1 and silicalite molecular sieves is explained by the reaction mechanisms proposed in Fig. 8.

The SiO_2 framework of silicalite-1 is not a good electron scavenger, and, since this material does not contain electron acceptors such as H^+ or Na^+, it is possible that the ejected electron readily neutralizes the newly created V centers and shifts the equilibrium strongly towards the left (mechanism I). This explains the low intensity for V centers observed in silicalite-1. In TS-1, however, a second mechanism by which V centers can be stabilized is reduction of Ti(IV) to Ti(III) by the ejected electron. This is consistent with the increase in V centers observed in TS-1, together with the formation of Ti(III), observed by ESR in comparison with silicalite-1. This provides further indirect evidence for the substitution of titanium into the TS-1 framework. As in zeolites, one expects two ESR signals for two V centers in TS-1 associated with Ti-O-Si and Si-O-Si units of the framework (22,23). However, the ESR spectrum observed does not distinguish these two possible types of V centers.

Several studies have been carried out on the coordination of framework titanium ions in relation to their role in catalytic transformations. Most of these studies deal with interactions between Ti(IV) and various molecules in the presence of hydrogen peroxide. Titanium silicates behave as Lewis acids due to the coordinatively unsaturated Ti(IV) ions. Adsorption of molecules such as ammonia, water, alcohol, and pyridine on TS-1 leads to changes in their optical spectra with respect to the spectra in the absence of adsorbates (29,30). All these changes are completely reversible. The well-known band at 960 cm^{-1} in the infrared spectra which is commonly associated with the presence of framework titanium, (2), shifts to higher wave numbers. New bands appear in the diffuse reflectance ultraviolet spectra,

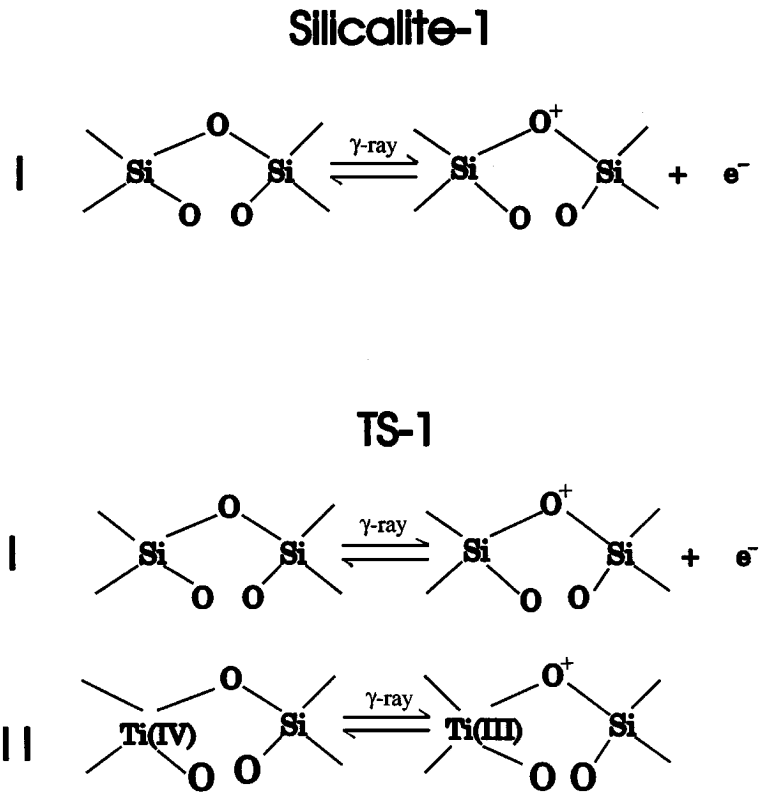

FIG. 8. Formation of V centers in silicalite-1 and TS-1 after γ-irradiation.

corresponding to charge-transfer transitions between the new ligands and the titanium ion (29). These new bands indicate a direct insertion of the ligands into the first coordination sphere of Ti(IV) which leads to an increase in the coordination number which is estimated to be about six for water adsorption (30). X-ray absorption techniques also give evidence for direct interaction of the ligands with the Ti(IV) ion (31,32). The intensities and half widths of the preedge X-ray absorption peaks in the presence of adsorbates correspond to Ti(IV) with a coordination number higher than tetrahedral. An increase of the distance between titanium and the atoms in its first coordination shell by 0.03 Å is observed for the adsorption of ammonia, methanol, and 2-propanol by EXAFS. This is explained by expansion of the Ti-O distance or by partial solvolysis of Ti-O-Si bridges and the formation of titanol groups (31,32).

Our ESR study of adsorption of various molecules such as water, methanol, and ethylene on TS-1 agrees in general with other spectroscopic studies (29–32) in that the coordination environment of the titanium changes significantly after adsorption, but our study differs in the actual number of molecules coordinating to titanium. Upon adsorption of D_2O on TS-1, the ESR signal of Ti(III) changes in line shape and g values, indicating a different environment for this ion from that of an activated sample. Several catalytic studies (1) suggest that by reaction with water, Ti-O-Si bonds are hydrolyzed to form TiOH and SiOH groups. This assumption is consistent with the parameters obtained from the ^{2}D ESEM spectrum of TS-1 after D_2O adsorption. The simulation showing two deuterium nuclei at distances of 3.0 Å and 3.5 Å seems consistent with the cleavage of Ti-O-Si bonds and the formation of TiOD and SiOD groups. A possible geometry for this structure is depicted in Fig. 9a. On the other hand, one expects nearly the same distance for the two deuterium nuclei if one D_2O coordinates with Ti(IV) without forming titanol and silanol groups as observed for the adsorption of D_2O on several other transition-metal-modified molecular sieves (33). Interaction of additional D_2O molecules with Ti(III) is unlikely as only two deuterium nuclei are observed in the vicinity of the Ti(III). Although Ti(III) still has four directly coordinated oxygens, the presence of a nearby silanol group alters the crystal field around the Ti(III). This probably explains the different ESR line shape and g value for Ti(III) after adsorption of D_2O.

Adsorption of CH_3OD on TS-1 again alters the ESR signal to Ti(III) from that of an activated sample. ^{2}D ESEM results of one deuterium interacting at 2.8 Å is consistent with coordination of one CH_3OD molecule to the Ti(III) ion. A possible geometry of this structure is shown in Fig. 9b. Here Ti(III) coordinates with five oxygens. The similar ESR signals observed for Ti(III) after adsorption of D_2O and

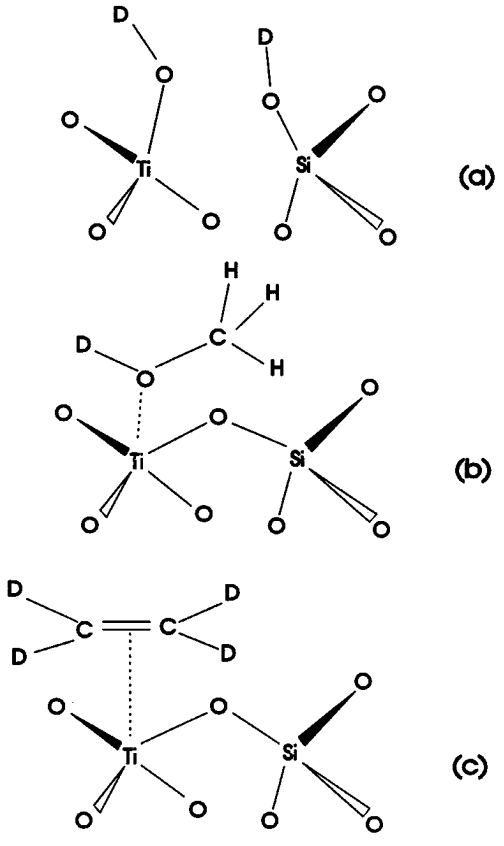

FIG. 9. Suggested coordination geometries of the Ti(III) complex obtained after adsorption of various molecules on TS-1 (a) after adsorption of D_2O, (b) after adsorption of CH_3OD, and (c) after adsorption of C_2D_4.

CH_3OD suggest that similar crystal fields exist for Ti(III) in these two cases.

With adsorbed C_2D_4, TS-1 shows an entirely different ESR signal for Ti(III). ^{2}D ESEM parameters of four deuteriums at 4.5 Å is consistent with one ethylene molecule coordinating with Ti(III) ion by π coordination. A possible geometry for this structure is shown in Fig. 9c. Similar π coordination of ethylene to titanium is suggested from various catalytic reactions (1). The interaction distance of 4.5 Å further indicates weak bonding between the ethylene molecule and Ti(III) ion. For adsorption of water, methanol, and ethylene, only one molecule of each coordinates with titanium in TS-1. Although this observation differs from other characterization results (29–32), it is consistent with models proposed from catalytic reactions (1,34). We suggest that the medium pore size of TS-1, together with the location of titanium in a framework tetrahedral site are both responsible for the observed behavior.

As discussed earlier the reversal of the g components of Ti(III) is a consequence of a change in the crystalline field bought about by interactions with additional ligands. Based on theoretical considerations, the reversal of the g values is possible when the crystalline field changes from tetrahedral to octahedral. In this study, the reversal of the g components of the Ti(III) species is observed when TS-1 is allowed to interact with molecules such as CO, H_2, and C_2H_4. The coordination sphere of Ti(III) in these cases involves one or more carbon or hydrogen ligands besides the four framework oxygens and may cause distortion of the crystalline field necessary for the reversal effect. On the other hand, when D_2O and CH_3OD are adsorbed on TS-1, no reversal of the g components was observed. The coordination sphere of Ti(III) in these cases involves only oxygen ligands and the associated crystalline field is modified to a lesser extent. Thus one expects only slight modifications of the ESR signal for Ti(III) before and after adsorption of the these molecules. This is what was observed in these two cases. In the specific case of adsorption with D_2O, the first coordination sphere of Ti(III) is modified only slightly from that of an activated sample due to the cleavage of Ti-O-Si bonds and the resultant formation of hydroxyl groups as suggested by Fig. 9a. This assumption is also consistent with the results of ^{2}D ESEM data on this sample.

CONCLUSIONS

Electron spin resonance and electron spin echo modulation spectroscopy are effective methods to study the reducibility and adsorbate interactions of Ti in titanosilicate TS-1 molecular sieve. Various reduction methods including γ-irradiation and treatment with H_2 or CO at high temperature are effective for reducing Ti(IV) to Ti(III) in TS-1. After dehydration, oxidation in O_2, and evacuation at 673 K (activation), TS-1 is γ-irradiated at 77 K and gives an axially symmetric ESR signal with $g_\parallel = 1.970$ and $g_\perp = 1.906$ of isolated Ti(III) centers. When activated TS-1 is treated with H_2 or CO at 673 K, an axially symmetric ESR signal with reversed g values is observed for Ti(III). When activated TS-1 is exposed to D_2O at room temperature and subsequently γ-irradiated at 77 K, a new and slightly anisotropic ESR signal with $g = 1.924$ is observed. Using ^{2}D ESEM, this species is identified as Ti(III)-$(OD)_1$ modified by interaction from nearby Si-OD groups. Adsorption of CH_3OD on activated TS-1 also produces a slightly anisotropic ESR signal with $g = 1.931$ for Ti(III) which is identified as Ti(III)-$(CH_3OD)_1$ from ^{2}D ESEM. The similar ESR signals observed for Ti(III) after water and methanol adsorption suggested a similar crystalline field around titanium in these two cases. Adsorption of C_2D_4 on activated TS-1 produces another new Ti(III) species with $g_\perp = 1.968$ and $g_\parallel = 1.910$ which is identified as Ti(III)-$(C_2D_4)_1$ from ^{2}D ESEM.

ACKNOWLEDGMENTS

This research was supported by the National Science Foundation, the Robert A. Welch Foundation, and the Texas Advanced Research Program.

REFERENCES

1. Notari, B., *Adv. Catal.* **41**, 253 (1996).
2. Vayssilov, G. N., *Catal. Rev.-Sci. Eng.* **39**, 209 (1997).
3. Khouw, C. B., Dart, C. B., Labinger, J. A., and Davis, M. E., *J. Catal.* **149**, 195 (1994).
4. Maspero, F., and Romano, U., *J. Catal.* **146**, 476 (1994).
5. Clerici, M. G., *Appl. Catal.* **68**, 249 (1991).
6. Clerici, M. G., Bellussi, G., and Romano, U., *J. Catal.* **129**, 159 (1991).
7. Reddy, J. S., Kumar, R., and Ratnasamy, P., *Appl. Catal.* **58**, L1 (1990).
8. Serrano, D. P., Li, H. X., and Davis, M. E., *J. Chem. Soc., Chem. Commun.*, 745 (1992).
9. Camblor, M. A., Corma, A., Martinez, A., and Perez-Pariente, J., *J. Chem. Soc., Chem. Commun.*, 589 (1992).
10. Ulagappan, N., and Krishnasamy, V., *J. Chem. Soc., Chem. Commun.*, 373 (1995).
11. Zahedi-Niaki, M. H., Joshi, P. N., and Kaliaguine, S., *in* "Progress in Zeolite and Microporous Materials" (H. Chon, S.-K. Ihm, and Y. S. Uh, Eds.), Studies in Surface Science and Catalysis, Vol. 105, p. 1013. Elsevier, Amsterdam, 1997.
12. Kresge, C. T., Leonovicz, M. E., Roth, W. J., Vartuli, J. C., and Beck, J. S., *Nature* **359**, 710 (1992).
13. Corma, A., Camblor, M. A., Esteve, P., Martinez, A., and Perez-Pariente, J., *J. Catal.* **145**, 151 (1994).
14. Koyano, K. A., and Tatsumi, T., *in* "Progress in Zeolite and Microporous Materials" (H. Chon, S.-K. Ihm, and Y. S. Uh, Eds.), Studies in Surface Science and Catalysis, Vol. 105, p. 93. Elsevier, Amsterdam, 1997.
15. Kuznicki, S. M., Thrush, K. A., Allen, F. M., Levine, S. M., Hamil, M. M., Hayhurst, D. T., and Mansour, M., *in* "Synthesis of Microporous Materials" (M. L. Occelli and H. Robson, Eds.), p. 427. Van Nostrand Reinhold, New York, 1992.
16. Tuel, A., Diab, J., Gelin, P., Dufaux, M., Dutel, J.-F., and Tarit, Y. B., *J. Mol. Catal.* **63**, 95 (1990).
17. Ghorbel, A., Tuel, A., Jorda, E., Ben Taarit, Y., and Naccache, C., *in* "Zeolites: A Refined Tool for Designing Catalytic Sites" (L. Bonneviot and S. Kaliaguine, Eds.), Studies in Surface Science and Catalysis, Vol. 97, p. 471. Elsevier, Amsterdam, 1995.
18. Prakash, A. M., Kurshev, V., and Kevan, L., *J. Phys. Chem. B* **101**, 9794 (1997).
19. Prakash, A. M., Sung-Suh, H. M., and Kevan, L., *J. Phys. Chem. B* **102**, 857 (1998).
20. Anderson, M. W., and Kevan, L., *J. Chem. Phys.* **87**, 1 (1987).
21. Millini, R., Massara, E. P., Perego, G., and Bellussi, G., *J. Catal.* **137**, 497 (1992).
22. Stamires, D. N., and Turkevich, J., *J. Am. Chem. Soc.* **86**, 757 (1964).
23. Abou-Kais, A., Vedrine, J. C., and Massardier, J., *J. Chem. Soc., Faraday Trans.* **71**, 1697 (1975).
24. Prakash, A. M., and Kevan, L., unpublished.
25. Kim, Y. M., and Bray, P. J., *J. Chem. Phys.* **53**, 716 (1970).
26. Weil, J. A., Bolton, J. R., and Wertz, J. E., "Electron Paramagnetic Resonance, Elementary Theory and Practical Applications," Chap. 8, p. 213. Wiley, New York, 1994.
27. Bencini, A., and Gatteschi, D., *in* "Transition Metal Chemistry" (G. A. Melson and B. N. Figgis, Eds.), Vol. 8, p. 1. Dekker, New York, 1982.
28. Yafaev, N. R., and Yablokov, Y. V., *Soviet Physics-Solid State* **4**, 1123 (1962).
29. Boccuti, M. R., Rao, K. M., Zecchina, A., Leofanti, G., and Petrini, G., *in* "Structure and Reactivity of Surfaces" (C. Morterra, A. Zecchina, and G. Costa, Eds.), Studies in Surface Science and Catalysis, Vol. 48, p. 133. Elsevier, Amsterdam, 1989.
30. Geobaldo, F., Bordiga, S., Zecchina, A., Giamello, E., Leofanti, G., and Petrini, G., *Catal. Lett.* **16**, 109 (1992).
31. Bordiga, S., Coluccia, S., Lamberti, C., Marches, L., Zecchina, A., Boscherini, F., Buffa, F., Genoni, F., Leofanti, G., Petrini, G., and Vlaic, G., *J. Phys. Chem.* **98**, 4125 (1994).
32. Davis, R. J., Liu, Z., Tabora, J. E., and Wielband, W. S., *Catal. Lett.* **34**, 101 (1995).
33. Prakash, A. M., and Kevan, L., *Langmuir* **13**, 5341 (1997).
34. Huybrechts, D. R. C., Buskens, P. L., and Jacobs, P. A., *J. Mol. Catal.* **71**, 129 (1992).